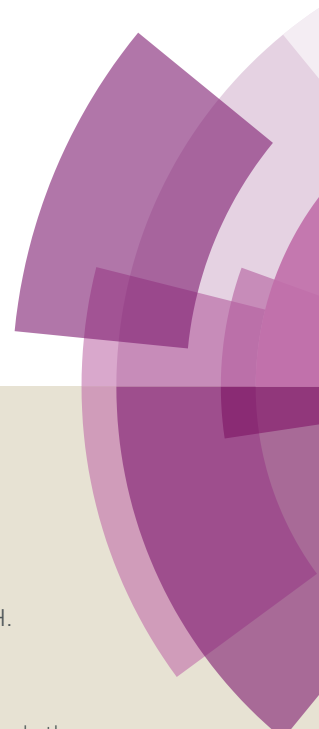


# Journal of Materials Chemistry C

Accepted Manuscript



This article can be cited before page numbers have been issued, to do this please use: X. Liu, C. Tao, H. Yu, B. Chen, Z. Liu, G. Zhu, Z. Zhao, L. Shen and B. Z. Tang, *J. Mater. Chem. C*, 2018, DOI: 10.1039/C7TC05535H.



This is an Accepted Manuscript, which has been through the Royal Society of Chemistry peer review process and has been accepted for publication.

Accepted Manuscripts are published online shortly after acceptance, before technical editing, formatting and proof reading. Using this free service, authors can make their results available to the community, in citable form, before we publish the edited article. We will replace this Accepted Manuscript with the edited and formatted Advance Article as soon as it is available.

You can find more information about Accepted Manuscripts in the [author guidelines](#).

Please note that technical editing may introduce minor changes to the text and/or graphics, which may alter content. The journal's standard [Terms & Conditions](#) and the ethical guidelines, outlined in our [author and reviewer resource centre](#), still apply. In no event shall the Royal Society of Chemistry be held responsible for any errors or omissions in this Accepted Manuscript or any consequences arising from the use of any information it contains.

## A new luminescent metal-organic framework based on dicarboxyl-substituted tetraphenylethene for efficient detection of nitro-containing explosives and antibiotics in aqueous media

Received 00th January 20xx,  
Accepted 00th January 20xx

DOI: 10.1039/x0xx00000x

www.rsc.org/

Xun-Gao Liu,<sup>\*a</sup> Chen-Lei Tao,<sup>a</sup> Huang-Qin Yu,<sup>a</sup> Bin Chen,<sup>b</sup> Zhen Liu,<sup>a</sup> Gen-Ping Zhu,<sup>a</sup> Zujin Zhao,<sup>\*b</sup> Liang Shen,<sup>\*a</sup> and Ben Zhong Tang<sup>bc</sup>

In this work, we synthesized a dicarboxyl-substituted tetraphenylethene (TPE) ligand, 4,4'-(1,2-diphenylethene-1,2-diyl)dibenzoic acid (H<sub>2</sub>BCTPE) with prominent aggregation-induced emission (AIE) feature. A two-fold interpenetrated luminescent metal-organic framework (LMOF) [Zn<sub>4</sub>O(BCTPE)<sub>3</sub>] (**1**) with Zn<sub>4</sub>O(CO<sub>2</sub>)<sub>6</sub> nodes is prepared by using the *trans*-isomer of H<sub>2</sub>BCTPE as a ligand, which shows a typical behavior of microporous materials and a high fluorescence quantum yield of 64.5%. The solvent free **1** is thermal stable, water stable and highly emissive. The suspension of solvent-free **1** in water exhibits high quenching efficiencies and low detection limits towards nitro-containing explosives (e.g. nitrobenzene, 4-nitrophenol, 2,4,6-trinitrophenol), and nitro-containing antibiotics (e.g. metronidazole and nitrofurazone). The solvent-free **1** can be a promising alternative to efficiently detect nitro-containing explosives and antibiotics in aqueous conditions.

### Introduction

Luminescent metal-organic frameworks (LMOFs), self-assembled from metal ions and organic legends, have shown giant potentials in chemical sensors, bioprobes, catalysis, and other diverse research frontiers.<sup>1-3</sup> The emissions of LMOFs can be produced from lanthanide metals, organic chromophores, metal-ligand charge transfer processes or guest molecules.<sup>4-6</sup> Recently, tetraphenylethene (TPE), a simple luminogen with prominent aggregation-induced emission (AIE) characteristic, is emerging as a popular building block to create LMOFs.<sup>7</sup> Immobilized in the rigid frameworks, TPE can fluoresce intensely and make major contributions to the emissions of LMOFs.<sup>8</sup> The strong emissions enable TPE-based LMOFs to serve as promising fluorescent sensors to detect volatile organic compounds, mycotoxins and nitro explosives in a turn-off mode.<sup>9,10</sup> Generally, TPE derivatives tetra-substituted with carboxyl or pyridyl groups, such as H<sub>4</sub>TCPE, H<sub>4</sub>ETTC, H<sub>8</sub>TDPEPE, tppe and TTPE, are utilized as ligands to construct LMOFs.<sup>11-14</sup> However, di-substituted TPE

derivatives were relatively rare in LMOFs, and there are only two examples: one is 4,4'-(2,2-diphenylethene-1,1-diyl)dibenzoic acid (DPEB) and the other is dipyridine-substituted (E)-1,2-diphenyl-1,2-bis(4-(pyridin-4-yl)phenyl)ethane (BPyTPE).<sup>15,16</sup> This is probably due to the difficulty lying in isolating pure *cis*- and *trans*-isomers from the products of McMurry coupling.<sup>17</sup> These ligands can connect with different metal ions to construct TPE-based LMOFs containing of 1D chains, paddle-wheel M<sub>2</sub>(COO)<sub>4</sub> units, Zn<sub>4</sub>O(CO<sub>2</sub>)<sub>6</sub> nodes or Zr<sub>6</sub> clusters.<sup>18-21</sup>

Nitro-containing antibiotics, metronidazole and nitrofurazone, are important medicines for mankind to prevent and treat certain diseases, as well as for resistance to bacterial infections in aquaculture. However, these medicines are already in the "list of drugs prohibited in animal foods" issued by National Bureau of Quality Inspection (AQSIQ) and Ministry of foreign trade and economic cooperation, because their residues in animals can be delivered to human body through the food chain. And long-term intake of these contaminated foods can cause a variety of diseases, like immunity decline, allergic reactions, hereditary genetic defects and various types of cancers.<sup>22,23</sup> At present, various expensive and complicated instruments, such as ion mobility spectrometry, high-performance liquid chromatography and other assays requiring sophisticated procedures are explored to detect metronidazole, nitrofurazone and so forth.<sup>24-27</sup> Therefore, as fluorescence sensors, LMOFs can provide a new alternative to readily detect these antibiotics with high sensitivity, short response time and high recyclability.<sup>28-32</sup>

In principle, Zn (II) and Zr (IV) metals can form Zn<sub>4</sub> clusters and Zr<sub>6</sub> clusters with carboxyl ligands, which are highly stable in water.<sup>33-36</sup> Linear organic carboxylic linkers are prone to

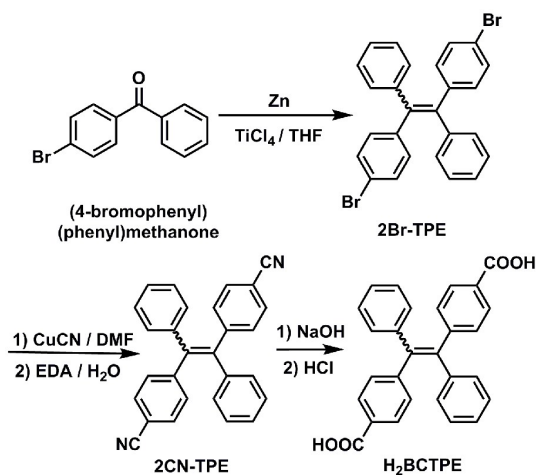
<sup>a</sup> College of Material, Chemistry and Chemical Engineering, Hangzhou Normal University, Hangzhou 310036, China. \*E-mail: xungaoliu@hznu.edu.cn; shenliang@hznu.edu.cn

<sup>b</sup> Center for Aggregation-Induced Emission, State Key Laboratory of Luminescent Materials and Devices, South China University of Technology, Guangzhou 510640, China. \*E-mail: mszjzhao@scut.edu.cn

<sup>c</sup> Department of Chemistry, Hong Kong Branch of Chinese National Engineering Research Center for Tissue Restoration and Reconstruction, The Hong Kong University of Science & Technology, Clear Water Bay, Kowloon, Hong Kong, China

† Electronic Supplementary Information (ESI) available: experimental details, crystallographic data, CIF files, thermal analysis, absorption and emission spectra, geometrical structures, PXRD patterns and fluorescence titration. See DOI: 10.1039/x0xx00000x

coordinate with Zn (II) ions to form  $[Zn_4(\mu_4-O)]^{6+}$  clusters with a 3D structure, such as isoreticular MOF (IRMOF) series.<sup>37-40</sup> With these considerations in mind, in this work, we use dicarboxyl-substituted TPE ( $H_2BCTPE$ ) to build a 3D LMOF  $[Zn_4O(BCTPE)_3]$  (**1**). Interestingly, only the *trans*-isomers of  $H_2BCTPE$  are incorporated in complex **1**, although  $H_2BCTPE$  are composed of *cis*- and *trans*-isomers produced from McMurry coupling.  $[Zn_4O(BCTPE)_3]$  is highly emissive and stable in water, and can function as an efficient sensor to detect nitro-containing explosives and antibiotics in aqueous media.



**Scheme 1.** Synthetic route to TPE-based ligand  $H_2BCTPE$ .

## Experimental section

### Synthesis

**4,4'-(1,2-Diphenylethene-1,2-diyl)dibenzoic acid ( $H_2BCTPE$ ).** A Sandmeyer reaction between 2Br-TPE and CuCN in tetrahydrofuran (THF) was performed to attach the CN moieties to TPE. To a 100 mL two-necked round-bottomed flask, 2Br-TPE (2 g, 5 mmol), CuCN (1.1 g, 12.2 mmol) and anhydrous THF (30 mL) were added. The mixture was heated at 160 °C for 3 days, and then cooled down to 90 °C.

Subsequently, ethylenediamine (4 mL) and  $H_2O$  (6 mL) were added into the mixture and heated to reflux for 3 h. After cooling down to room temperature, 4,4'-(1,2-diphenylethene-1,2-diyl)dibenzonitrile (2CN-TPE) was obtained by extracting with dichloromethane (DCM) and drying over anhydrous magnesium sulfate. After filtration and solvent evaporation, crude 2CN-TPE underwent hydrolysis reaction carried out in ethylene glycol (40 mL) containing NaOH (0.4 g, 10 mmol) at 200 °C for 3 days. Then, HCl (1 mol/L, 10 mL) solution was added carefully to quench the reaction after cooling down to room temperature. Pale brown solid of  $H_2BCTPE$  (a mixture of *cis*- and *trans*-isomers) was obtained in 45% overall yield after filtering, washing with water for three times and air drying.  $^1H$  NMR (600 MHz, DMSO- $d_6$ ),  $\delta$  (TMS, ppm): 12.97 (s, 2H), 7.75 (m, 4H), 7.15 (m, 8H), 7.19 (d, 2H), 6.99 (d, 4H).  $^{13}C$  NMR (150 MHz, DMSO- $d_6$ ),  $\delta$  (TMS, ppm): 166.98, 147.37, 142.16, 140.91, 130.74, 130.55, 128.91, 128.84, 128.05, 127.96, 127.02. IR: (KBr pellet,  $cm^{-1}$ ): 3056 (m), 1700 (s), 1603 (s), 1563 (m), 1442 (m), 1409 (s), 1311 (m), 1273 (s), 1177 (s), 1105 (m), 1074 (w), 1017 (m), 859 (m), 761 (m), 745 (s), 699 (m). ESI (FAB):  $m/z$  = 421.136  $[M + H]^+$ .

**$[Zn_4O(BCTPE)_3]$  (**1**).**  $Zn(NO_3)_2 \cdot 6H_2O$  (10 mg, 34 mmol),  $H_2BCTPE$  (8 mg, 19 mmol) and *N,N*-dimethylformamide (DMF, 2 mL) were added in a 10 mL screw-capped vial. The solids were ultrasonically dissolved and kept at 100 °C for 2 days. After the reaction mixture was cooled down to room temperature, the transparent pale yellow cube crystals were harvested via filtrating and washed with DMF for three times. Yield: 35%. IR: (KBr pellet,  $cm^{-1}$ ): 1660 (s), 1602 (s), 1538 (s), 1408 (s), 787 (w), 755 (m), 720 (w), 701 (m).

Complex **1** was soaked in DCM for 3 days, during which time DCM was decanted and refreshed every day, and then dried under a dynamic vacuum at room temperature for 3 h to obtain solvent-free **1**. Anal. Calcd for  $C_{28}H_{18}O_{4.33}Zn_{1.33}$ : C, 65.76; H, 3.52; O, 13.56%; Found: C, 65.20; H, 3.36; O, 13.63%. IR: (KBr pellet,  $cm^{-1}$ ): 1600 (s), 1548 (s), 1413 (s), 785 (m), 754 (m), 721 (w), 700 (m).

### Fluorescence titration.

Solvent-free **1** was added to water, and the mixture was kept under vortex for 30 s to form a suspension with a concentration of 0.3

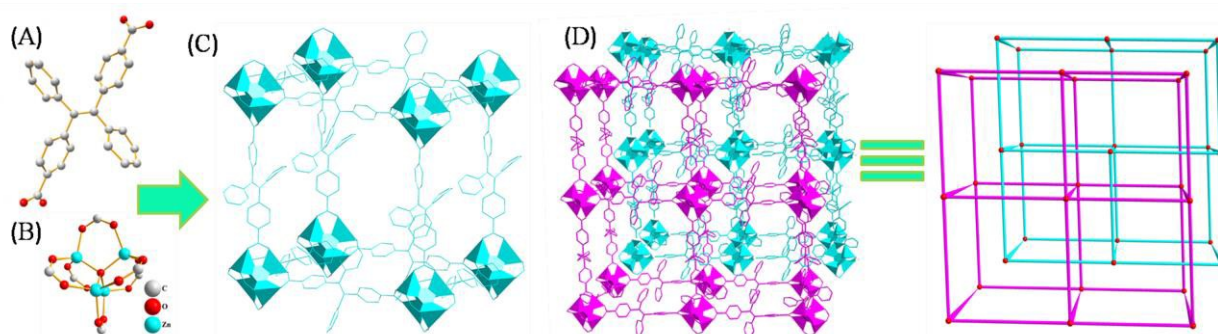


**Fig. 1** (A) Structure of  $BCTPE^{2-}$  ligand in complex **1**. (B) Structure of  $Zn_4O(CO_2)_6$  node in complex **1**. (C) Cubic structure of single net of complex **1**. (D) Overall crystal structure of complex **1** (two-fold interpenetration and 1D pore). Hydrogen atoms are omitted, and solvent molecules are removed by using the SQUEEZE routine of PLATON for clarity.

mg/mL. Since nitrobenzene (NB) is almost insoluble in water, we chose methanol as dispersant for detection. The fluorescence titration was performed by adding analytes to solvent-free **1** suspension and the photoluminescence (PL) spectra of the suspension were recorded on a Perkin-Elmer LS 55 spectrofluorometer. By setting the excitation wavelength at 365 nm, the emission spectra from 400 to 700 nm were collected at room temperature.

## Results and discussion

### Topological analysis

Single-crystal X-ray diffraction analysis revealed that complex **1** crystallizes in the trigonal space group  $R\bar{3}$  (Table S1). Its framework consists of  $[Zn_4(\mu_4-O)]^{6+}$  cluster cores, which are connected with six carboxylate groups from six (*trans*)- $H_2BCTPE$  ligands (Fig. 1A) to form a classic  $Zn_4O(CO_2)_6$  node (Fig. 1B). The bond lengths of Zn-O are between 1.920–1.974 Å, tallying with that of reported octahedral oxozinc clusters compounds. The  $Zn_4O(CO_2)_6$  nodes are further linked by  $BCTPE^{2-}$  with co-shared carboxylate groups to generate a cubic 3D framework, and the length of each edge is 19.47 Å (Fig. 1C). A two-fold interpenetrated framework is observed for the entire structure (Fig. 1D). The further investigation of geometrical conformation for  $BCTPE^{2-}$  in complex **1** shows that the average dihedral angles between phenyl rings and the ethene stator are around 55° (Fig. S1). There are C–H $\cdots\pi$  interactions with a distance of 3.24 Å formed between adjacent phenyl rings of TPE moieties (Fig. S2). The pore volume of complex **1** is 10458.4 Å<sup>3</sup>,

corresponding to a void of around 47.4% per unit cell (22066.0 Å<sup>3</sup> in total), almost twice larger than that of classic reported MOF-5 (12860.0 Å<sup>3</sup> in total) as calculated by using the PLATON.<sup>41</sup>

### General characterizations.

Powder X-ray diffraction patterns (PXRD) of complex **1** and solvent-free **1** confirmed that the bulk samples are of high purity and the structure of solvent-free **1** is retained without collapses. Moreover, solvent-free **1** shows good stability in H<sub>2</sub>O and methanol as proved by PXRD patterns, which is the same as other MOFs with octahedral oxozinc clusters (Fig. 2). Thermogravimetric analysis (TGA) of complex **1** reveals 25% initial weight loss after heating from 30 to 180 °C in nitrogen stream, which is attributed to solvent removal. A second sharp weight loss (~50%) occurs at 450–500 °C, corresponding to the decomposition of the framework. However, solvent-free **1** only starts to lose weight at 450 °C (Fig. S3), indicative of the absence of solvent molecules.

To investigate the permanent porosity, solvent-free **1** was activated at 333 K under vacuum for 7 h. The nitrogen sorption isotherm for solvent-free **1** at 77 K shows a typical behavior of microporous materials, that is a steep nitrogen uptake at low relative pressure ( $P/P_0 < 0.01$ ) (Fig. 3). The Brunauer–Emmett–Teller and Langmuir specific surface areas of solvent-free **1** estimated by nitrogen sorption isotherms are 530.6 and 682.6 m<sup>2</sup>/g, respectively.

### Optical properties.

$H_2BCTPE$  shows a broad absorption band around 330 nm in dilute THF solution, which mainly stems from the  $\pi$ - $\pi^*$  transition of the

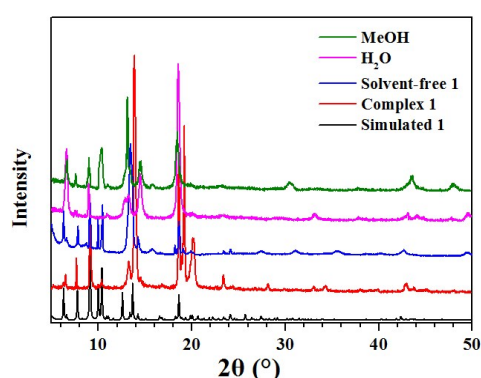


**Fig. 2** The PXRD patterns of simulated **1**, complex **1**, solvent-free **1** and solvent-free **1** after being soaked in H<sub>2</sub>O and MeOH, respectively.

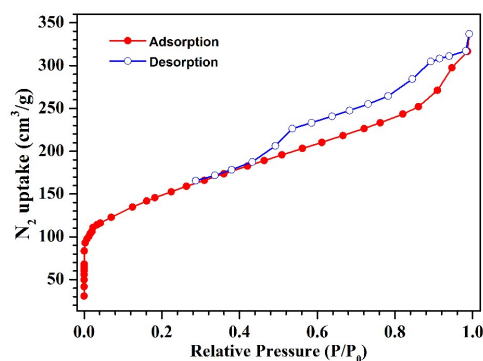


**Fig. 3** Nitrogen sorption isotherms of solvent-free **1** at 77 K.

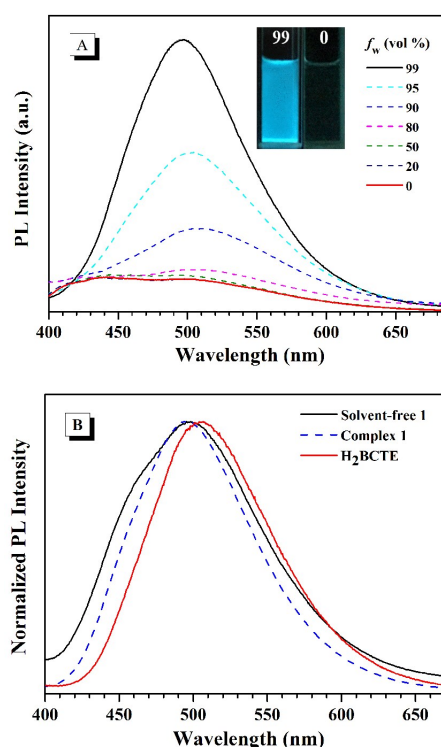


**Fig. 4** (A) Photoluminescence (PL) spectra of  $H_2BCTPE$  in THF/water mixtures with various water fractions ( $f_w$ ). Inset: photos of  $H_2BCTPE$  in THF/water mixtures ( $f_w = 99$  and 0 vol%). (B) Solid-state PL spectra of complex **1**, solvent-free **1** and  $H_2BCTPE$ .

conjugated molecular backbone (Fig. S4). H<sub>2</sub>BCTPE, like most TPE derivatives, exhibits prominent AIE attribute. As depicted in Fig. 4A, it shows faint emission in THF solution or THF/water mixture with a water fraction ( $f_w$ , vol%) less than 80%. But its emission intensity is rapidly enhanced at a higher  $f_w$ . H<sub>2</sub>BCTPE emits strong fluorescence with an emission peak at 503 nm in the aggregated state. The fluorescence quantum yield ( $\Phi_F$ ) of H<sub>2</sub>BCTPE is 24.5% in solid, which is amongst those of carboxyl-substituted TPE derivatives.<sup>42</sup> The  $\Phi_F$  of H<sub>2</sub>BCTPE is much higher than that of tetracarboxyl-substituted TPE in solid (0.8%).<sup>11c</sup> Compared with H<sub>2</sub>BCTPE, complex **1** and solvent-free **1** show slightly blue-shifted emission peaks at 495 and 499 nm, respectively (Fig. 4B), owing to the more rigidified molecular structure and thus reduced reorganization energy.<sup>43-45</sup> The  $\Phi_F$ s of solvent-free **1** and complex **1** are 44.1% and 64.5%, respectively, much higher than that of H<sub>2</sub>BCTPE (24.5%) in solid. The fluorescence lifetimes ( $\tau$ ) of H<sub>2</sub>BCTPE solid, solvent-free **1** and complex **1** are 4.31, 3.83 and 3.78 ns, respectively, which agree well with the tendency of  $\Phi_F$ s. This is also caused by the more rigidified molecular structure of TPE moiety when embedded into the framework. Complex **1** has a higher  $\Phi_F$  solvent-free **1**, probably owing to the formation of C–H... $\pi$  interaction between TPE moieties and trapped solvent molecules. The collective forces can further restrict molecular motions and prevent excited-state structure distortion of TPE moieties in the framework, and thus give rise to a higher  $\Phi_F$ .<sup>16, 18a, 46</sup>

#### Nitro explosives detection.

Solvent-free **1** is dispersed into H<sub>2</sub>O, followed by 30 seconds vortex to form a stable suspension, which emits strongly at 489 nm (Fig.

S5). The bright emission and good water dispersion of solvent-free **1** inspired us to explore its potential applications in detection of nitro-containing explosives, such as nitrobenzene (NB), 4-nitrophenol (NP) and 2,4,6-trinitrophenol (TNP) in aqueous media. The quenching efficiency (QE) is estimated using the formula of  $(I_0 - I)/I_0$  ( $I_0$  is initial fluorescence intensity and  $I$  is fluorescence intensity after adding guest molecules).<sup>47,48</sup> In the presence of 50 ppm analytes, the emission intensity of solvent-free **1** declines to different extents. The QE of NB is 7%, while those of NP and TNP are increased to 76% and 90%, respectively (Fig. 5A to 5C). To examine the sensitivity of solvent-free **1** dispersed in water towards nitro-containing explosives in detail, the fluorescence titrations with gradual additions of NB, NP and TNP were performed and the changes in emission intensity was monitored (Fig. S6, S8 and S10). The linear quenching ranges of solvent-free **1** suspension upon the additions of NB, NP and TNP are showed in Fig. S7B, S9B and S11B. From a ratio of  $3\sigma/k$  ( $\sigma$ : standard deviation;  $k$ : slope), the limits of detection (LOD) are calculated to be 10, 0.13 and 0.1 ppm for NB, NP and TNP, respectively. The detection limits are further confirmed by the fluorescence titrations of these analytes at low concentrations (Fig. S6 to S11). Hydrogen bonding interactions (e.g.) between the hydroxyl of analytes and the oxygen of BCTPE<sup>2-</sup> may bring analytes closer to solvent-free **1** and facilitate interactions between them.<sup>49</sup>

#### Antibiotics detection.

According to Announcement No. 235 of the Ministry of Agriculture of the People's Republic of China, nitro-containing antibiotics, metronidazole and nitrofurazone, cannot exist in Food-Producing

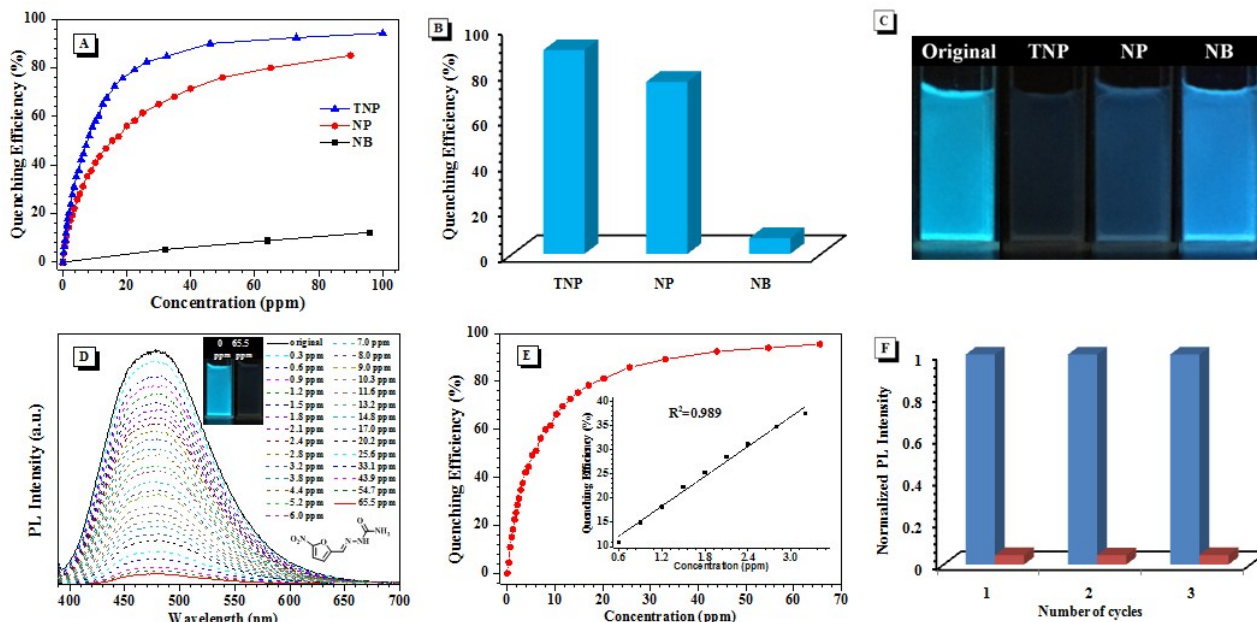


**Fig. 5** (A) Correlation between the quenching efficiency and concentration of TNP, NP and NB within 100 ppm. (B) The quenching efficiency of solvent-free **1** suspension by 50 ppm TNP, NP and NB ( $\lambda_{ex}$  = 365 nm). (C) Photos of solvent-free **1** suspension and solvent-free **1** suspension with TNP, NP and NB (50 ppm). (D) Fluorescence titration of solvent-free **1** in water suspension with varied concentrations of nitrofurazone ( $\lambda_{ex}$  = 365 nm). Inset: photos of solvent-free **1** in water suspension with 0 and 65.5 ppm nitrofurazone. (E) Correlation between the quenching efficiency and concentration of nitrofurazone. Inset: the linear relationship of fitting (0–3 ppm). (F) Reproducibility of the quenching ability of solvent-free **1** with nitrofurazone. (The blue bars represent the initial fluorescence intensity, and the red bars represent the intensity upon the addition of 65 ppm nitrofurazone.)

Animals. Hence, solvent-free **1** dispersed in water is used to detect these antibiotics. The emission intensity of solvent-free **1** is decreased drastically by 93% of the original intensity at 50 ppm of nitrofurazone, and 50% at the same concentration of metronidazole (Fig. S12), which are discernible by the naked eye. As shown in Fig. 5, the emission solvent-free **1** starts to decrease upon the addition of 0.3 ppm nitrofurazone and 2.0 ppm metronidazole. The lowest concentrations for complete quenching (QE = 97%) are 65 ppm for nitrofurazone and 900 ppm for metronidazole. The LODs of nitrofurazone and metronidazole are calculated to be 0.1 and 0.6 ppm, respectively, which are confirmed by fluorescence titrations at low concentrations (Fig. S13 to S16). Solvent-free **1** exhibits higher sensitivities towards nitrofurazone and metronidazole than NB (10 ppm), and the LODs of antibiotics are comparable to that of TNP (0.1 ppm). In addition, solvent-free **1** can be reused by centrifuging the suspension and washing with water for several times.<sup>50</sup> Obviously, solvent-free **1** can meet the requirements in detection of antibiotics metronidazole and nitrofurazone. To understand the sensing mechanism, the HOMO and LUMO energy levels of NB, NP, TNP, nitrofurazone, metronidazole and H<sub>2</sub>BCTPE are investigated theoretically.<sup>51</sup> It is found that the excited-state electron transfer from the higher LUMO of H<sub>2</sub>BCTPE (-1.94 eV) to those of analyte (<-2.22 eV) may occur under photon excitation, resulting in severe fluorescence quenching (Fig. S17). Therefore, the photon-induced electron transfer (PET) could play a crucial role in the detection of these analytes. On the other hand, the fluorescence resonance energy transfer (FRET) hardly contributes to the fluorescence quenching because of less overlap between the absorption spectra of nitro-containing analytes and emission spectrum of solvent-free **1** (Fig. S18).

## Conclusions

In summary, a new dicarboxyl-substituted, AIE-active TPE derivative, H<sub>2</sub>BCTPE, is designed and synthesized. Based on H<sub>2</sub>BCTPE, we have developed a two-fold interpenetrated LMOF [Zn<sub>4</sub>O(BCTPE)<sub>3</sub>] (**1**) with a classical Zn<sub>4</sub>O(CO<sub>2</sub>)<sub>6</sub> nodes. Although H<sub>2</sub>BCTPE is a mixture of *cis*- and *trans*-isomers obtained from McMurry coupling, only *trans*-isomer of H<sub>2</sub>BCTPE is spontaneously incorporated complex **1**. Solvent-free **1** is highly emissive, thermal stable and water stable, and exhibits a typical behavior of microporous materials. The emission of solvent-free **1** can be quenched efficiently by nitro-containing explosives, and a reversible method to sensitively and quantitatively detect trace NP and TNP in water is established. In addition, solvent-free **1** also shows good performance in the detection of antibiotics with low LODs of 0.6 ppm and 0.1 ppm for metronidazole and nitrofurazone, respectively, in aqueous conditions. These results demonstrate that solvent-free **1** is a promising candidate for the detection of nitro-containing explosives and antibiotics in aqueous environments. Further studies of detecting other drugs as well as heavy metal pollutants with TPE-based LMOFs are in progress.

## Conflicts of interest

There are no conflicts to declare.

## Acknowledgements

We thank for financial support from the National Natural Science Foundation of China (21788102 and 21671051), the Zhejiang Provincial Natural Science Foundation of China (LY15B010006 and LY16B010003) and the Innovative Research Team in Chinese University (IRT 1231). X.-G. Liu thanks the financial support from climb project–phase II for discipline construction project of Hangzhou normal university. Z.Z. thanks the financial support from Guangdong Natural Science Funds for Distinguished Young Scholar (2014A030306035). We also thank Dr Zaichao Zhang for his assistance in crystallographic analysis.

## Notes and references

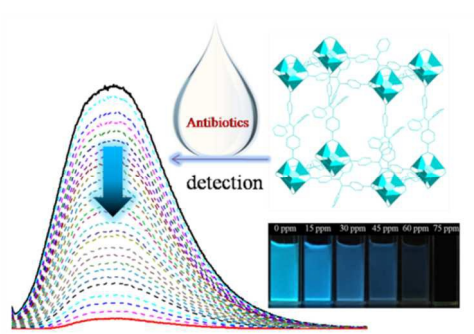
- 1 Y. Cui, Y. Yue, G. Qian and B. Chen, *Chem. Rev.*, 2012, **112**, 1126.
- 2 W. P. Lustig, S. Mukherjee, N. D. Rudd, A. V. Desai and J. Li, *Chem. Soc. Rev.*, 2017, **46**, 3242.
- 3 (a) Y. Cui, B. Li, H. He, W. Zhou, B. Chen and G. Qian, *Acc. Chem. Res.*, 2016, **49**, 483; (b) L. E. Kreno, K. Leong, O. K. Farha, M. Allendorf, R. P. V. Duyne and J. T. Hupp, *Chem. Rev.*, 2012, **112**, 1105.
- 4 J. Heine and K. Muller-Buschbaum, *Chem. Soc. Rev.*, 2013, **42**, 9232.
- 5 X. Yan, T. R. Cook, P. Wang, F. Huang and P. J. Stang, *Nat. Chem.*, 2015, **7**, 342.
- 6 J. Mei, N. L. C. Leung, R. T. K. Kwok, J. W. Y. Lam and B. Z. Tang, *Chem. Rev.*, 2015, **115**, 11718.
- 7 (a) S. Dalapati, C. Gu and D. Jiang, *Small*, 2016, **47**, 6513; (b) V. W.-W. Yam, V. K.-M. Au and S. Y.-L. Leung, *Chem. Rev.*, 2015, **115**, 7589.
- 8 (a) L. Ma, X. Feng, S. Wang and B. Wang, *Mater. Chem. Front.*, 2017, **1**, 2474; (b) Y. Guo, X. Feng, T. Han, S. Wang, Z. Lin, Y. Dong and B. Wang, *J. Am. Chem. Soc.*, 2014, **136**, 15485; (c) Z. Zhao, J. W. Y. Lam and B. Z. Tang, *J. Mater. Chem.*, 2012, **22**, 23726.
- 9 Z. Hu, B. J. Deibert and J. Li, *Chem. Soc. Rev.* 2014, **43**, 5815.
- 10 F.-Y. Yi, D. Chen, M.-K. Wu, L. Han and H.-L. Jiang, *ChemPlusChem*, 2016, **81**, 675.
- 11 (a) N. B. Shustova, T.-C. Ong, A. F. Cozzolino, V. K. Michaelis, R. G. Griffin and M. Dincă, *J. Am. Chem. Soc.*, 2012, **134**, 15061; (b) N. B. Shustova, A. F. Cozzolino and M. Dincă, *J. Am. Chem. Soc.*, 2012, **134**, 19596; (c) N. B. Shustova, B. D. McCarthy and M. Dincă, *J. Am. Chem. Soc.* 2011, **133**, 20126.
- 12 S. L. Jackson, A. Rananaware, C. Rix, S. V. Bhosale and K. Latham, *Cryst. Growth Des.*, 2016, **16**, 3067.
- 13 (a) B. J. Deibert, E. Velasco, W. Liu, S. J. Teat, W. P. Lustig and J. Li, *Cryst. Growth Des.*, 2016, **16**, 4178; (b) Z. Hu, W. P. Lustig, J. Zhang, C. Zheng, H. Wang, S. J. Teat, Q. Gong, N. D. Rudd and J. Li, *J. Am. Chem. Soc.*, 2015, **137**, 16209.
- 14 (a) X. Liu, J. C. Steele and X.-Z. Meng, *Environ. Pollut.*, 2017, **223**, 161; (b) Z. Zhou, C. He, J. Xiu, L. Yang and C. Duan, *J. Am. Chem. Soc.*, 2015, **137**, 15066.
- 15 M. Zhang, G. Feng, Z. Song, Y.-P. Zhou, H.-Y. Chao, D. Yuan, T. Y. Tan, Z. Guo, Z. Hu, B. Z. Tang, B. Liu and Dan Zhao, *J. Am. Chem. Soc.*, 2014, **136**, 7241.
- 16 C.-L. Tao, B. Chen, X.-G. Liu, L.-J. Zhou, X.-L. Zhu, J. Cao, Z.-G. Gu, Z. Zhao, L. Shen and B. Z. Tang, *Chem. Commun.*, 2017, **53**, 9975.
- 17 J. Shi, W. Zhao, C. Li, Z. Liu, Z. Bo, Y. Dong, T. Dong and B. Z. Tang, *Chin. Sci. Bull.*, 2013, **58**, 2723.
- 18 (a) Z. Wei, Z.-Y. Gu, R. K. Arvapally, Y.-P. Chen, J. R. N. McDougald, F. I. Joshua, A. A. Yakovenko, D. Feng, M. A. Omary and H.-C. Zhou, *J. Am. Chem. Soc.*, 2014, **136**, 8269; (b) Q. Gong, Z. Hu, B. J. Deibert, T. J. Emge, S. J. Teat, D.

- Banerjee, B. Mussman, N. D. Rudd and J. Li, *J. Am. Chem. Soc.*, 2014, **136**, 16724.
- 19 Y. Wang, B. Yuan, Y.-Y. Xu, X.-G. Wang, B. Ding and X.-J. Zhao, *Chem. Eur. J.*, 2015, **21**, 2107.
- 20 X.-G. Liu, H. Wang, B. Chen, Y. Zou, Z.-G. Gu, Z. Zhao and L. Shen, *Chem. Commun.*, 2015, **51**, 1677.
- 21 N. B. Shustova, A. F. Cozzolino and M. Dincă, *J. Am. Chem. Soc.* 2012, **134**, 19596.
- 22 X. Wang, O. S. Wolfbeis and R. J. Meier, *Chem. Soc. Rev.*, 2013, **42**, 7834.
- 23 K. Kümmerer, *Chemosphere*, 2009, **75**, 417.
- 24 Q.-Q. Zhang, G.-G. Ying, C.-G. Pan, Y.-S. Liu and J.-L. Zhao, *Environ. Sci. Technol.*, 2015, **49**, 6772.
- 25 P. W. Seo, N. A. Khan and S. H. Jhung, *Chem. Eng. J.*, 2017, **315**, 92.
- 26 N. Lu, T. Wang, P. Zhao, L. Zhang, X. Lun, X. Zhang and X. Hou, *Anal. Bioanal. Chem.*, 2016, **408**, 8515.
- 27 M. Ibrahim, R. Sabouni and G. Hussein, *Curr. Med. Chem.*, 2017, **24**, 193.
- 28 B. Wang, X.-L. Lv, D. Feng, L.-H. Xie, J. Zhang, M. Li, Y. Xie, J.-R. Li and H.-C. Zhou, *J. Am. Chem. Soc.*, 2016, **138**, 6204.
- 29 F. Zhang, H. Yao, Y. Zhao, X. Li, G. Zhang and Y. Yang, *Talanta*, 2017, **174**, 660.
- 30 D. Zhao, X.-H. Liu, Y. Zhao, P. Wang, Y. Liu, M. Azam, S. I. Al-Resayes, Y. Lu and W.-Y. Sun. *J. Mater. Chem. A*, 2017, **5**, 15797.
- 31 F. Zhang, H. Yao, T. Chu, G. Zhang, Y. Wang and Y. Yang, *Chem. Eur. J.*, 2017, **23**, 10293.
- 32 N. S. Bobbitt, M. L. Mendonca, A. J. Howarth, T. Islamoglu, J. T. Hupp, O. K. Farha and R. Q. Snurr, *Chem. Soc. Rev.*, 2017, **46**, 3357.
- 33 (a) W. Li, X. Qi, C.-Y. Zhao, X.-F. Xu, A.-N. Tang and D.-M. Kong, *ACS Appl. Mater. Interfaces*, 2017, **9**, 236; (b) Q. Zhang, J. Su, D. Feng, Z. Wei, X. Zou and H.-C. Zhou, *J. Am. Chem. Soc.*, 2015, **137**, 10064.
- 34 B. Wang, Q. Yang, C. Guo, Y. Sun, L.-H. Xie and J.-R. Li, *ACS Appl. Mater. Interfaces*, 2017, **9**, 10286.
- 35 B.-L. Hou, D. Tian, J. Liu, L.-Z. Dong, S.-L. Li, D.-S. Li and Y.-Q. Lan, *Inorg. Chem.*, 2016, **55**, 10580.
- 36 F.-L. Yuan, Y.-Q. Yuan, M.-Y. Chao, D. J. Young, W.-H. Zhang and J.-P. Lang, *Inorg. Chem.*, 2017, **56**, 6522.
- 37 R. J. Marshall, Y. Kalinovsky, S. L. Griffin, C. Wilson, B. A. Blight and R. S. Forgan, *J. Am. Chem. Soc.* 2017, **139**, 6253.
- 38 L. Li, X. Cao and R. Huang, *Chin. J. Chem.*, 2016, **34**, 143.
- 39 M. Eddaoudi, J. Kim, N. Rosi, D. Vodak, J. Wachter, M. O'Keeffe and O. M. Yaghi, *Science*, 2002, **98**, 469.
- 40 C. A. Bauer, T. V. Timofeeva, T. B. Settersten, B. D. Patterson, V. H. Liu, B. A. Simmons and M. D. Allendorf, *J. Am. Chem. Soc.*, 2007, **129**, 7136.
- 41 Spek, A. L. PLATON: A Multipurpose Crystallographic Tool; Utrecht University: Utrecht, The Netherlands, 2001.
- 42 J. Mei, Y. Hong, J. W. Y. Lam, A. Qin, Y. Tang and B. Z. Tang, *Adv. Mater.* 2014, **26**, 5429.
- 43 (a) S. Yuan, Y.-K. Deng and D. Sun, *Chem. Eur. J.*, 2014, **20**, 10093; (b) Q. Wu, T. Zhang, Q. Peng, D. Wang and Z. Shuai, *Phys. Chem. Chem. Phys.*, 2014, **16**, 5545.
- 44 (a) L. Zhou, Z.-G. Wang, H.-Y. Dong, K. Zhao, Y.-J. Hu, Z.-J. Gao, S.-N. Tie and H.-G. Zheng, *Inorg. Chem. Commun.*, 2017, **78**, 1; (b) F. Bu, R. Duan, Y. Xie, Y. Yi, Q. Peng, R. Hu, A. Qin, Z. Zhao and B. Z. Tang, *Angew. Chem. Int. Ed.*, 2015, **54**, 14492; (c) W. Luo, H. Nie, B. He, Z. Zhao, Q. Peng and B. Z. Tang, *Chem. Eur. J.*, 2017, DOI: 10.1002/chem.201704182.
- 45 D. Jonckheere, J. A. Steele, B. Claes, B. Bueken, L. Claes, B. Lagrain, M. B. J. Roeffaers and D. E. D. Vos, *ACS Appl. Mater. Interfaces*, 2017, **9**, 30064.
- 46 Y. Fushimi, M. Koinuma, Y. Yasuda, K. Nomura and M. S. Asano, *Macromolecules*, 2017, **50**, 1803.
- 47 S.-Y. Zhang, W. Shi, P. Cheng and M. J. Zaworotko, *J. Am. Chem. Soc.*, 2015, **137**, 12203. DOI: 10.1039/C7TC05535H
- 48 X.-G. Hou, Y. Wu, H.-T. Cao, H.-Z. Sun, H.-B. Li, G.-G. Shan and Z.-M. Su, *Chem. Commun.*, 2014, **50**, 6031.
- 49 (a) Y. Zhang, B. Li, H. Ma, L. Zhang and W. Zhang, *J. Mater. Chem. C*, 2017, **5**, 4661; (b) J. Qin, B. Ma, X. Liu, H. Lu, X. Dong, S. Zang and H. Hou, *J. Mater. Chem. A*, 2015, **3**, 12690; (c) Q. Tan, Y. Wang, X. Guo, H. Liu and Z. Liu, *RSC Adv.*, 2016, **6**, 61725; (d) Z. Sun, Y. Li, Y. Ma and L. Li, *Dyes Pigm.*, 2017, **146**, 263; (e) R. Dalapati and S. Biswas, *Sensor Actuat B: Chem.*, 2017, **239**, 759.
- 50 W.-M. Chen, X.-L. Meng, G.-L. Zhuang, Z. Wang, M. Kurmoo, Q.-Q. Zhao, X.-P. Wang, B. Shan, C.-H. Tung and D. Sun, *J. Mater. Chem. A*, 2017, **5**, 13079.
- 51 (a) Y. Zhao, X. Xu, L. Qiu, X. Kang, L. Wen and B. Zhang, *ACS Appl. Mater. Interfaces*, 2017, **9**, 15164; (b) S. S. Nagarkar, A. V. Desai and S. K. Ghosh, *Chem. Commun.*, 2014, **50**, 8915; (c) M. Gao, Y. Wu, B. Chen, B. He, H. Nie, T. Li, F. Wu, W. Zhou, J. Zhou and Z. Zhao, *Polym. Chem.*, 2015, **6**, 7641; (d) D. Chen, J. Tian, Z. Wang, C. Liu, M. Chen and M. Du, *Chem. Commun.*, 2017, **53**, 10668.

# A new luminescent metal-organic framework based on dicarboxyl-substituted tetraphenylethene for efficient detection of nitro-containing explosives and antibiotics in aqueous media

Xun-Gao Liu,<sup>\*a</sup> Chen-Lei Tao,<sup>a</sup> Huang-Qin Yu,<sup>a</sup> Bin Chen,<sup>b</sup> Zhen Liu,<sup>a</sup> Gen-Ping Zhu,<sup>a</sup> Zujin Zhao,<sup>\*b</sup> Liang Shen,<sup>\*a</sup> and Ben Zhong Tang<sup>bc</sup>

## Table of contents entry



A tetraphenylethene-based luminescent metal-organic framework with high fluorescence quantum yield efficiently and quantitatively detected trace nitro-containing antibiotics in aqueous media.